International Journal of Coal Science & Technology (2024) 11:82
https://doi.org/10.1007/s40789-024-00732-7

RESEARCH

Study on the flow field of multi-phase coupling slag discharge and the influencing factors of slag discharge effect in gas lift reverse circulation of drilling shaft sinking

Longhui Guo[1] · Hua Cheng[1,2,3] · Zhishu Yao[1] · Chuanxin Rong[1] · Guang Yang[4] · Xiaoyun Wang[1] · Yu Fang[1] · Bao Xie[1]

Received: 16 September 2023 / Revised: 15 January 2024 / Accepted: 27 August 2024

Abstract
Combined with the advanced drilling of the central return air shaft in Kekegai Coal Mine, the distribution law of slag discharge flow field by drilling method and the influencing factors of slag discharge effect are studied. Firstly, the numerical model of gas–liquid–solid coupling slag discharge is established by CFD-DEM (computational fluid dynamics coupled discrete element method). Then, the flow field distribution law of the site slag outlet layout model and the optimization model is compared and analyzed. Finally, the influence of drilling parameters on slag discharge effect is studied. The results show that the best arrangement of slag suction ports is: the number is two, the length-diameter ratio is 0.4, the area ratio is 1, and the total area ratio is 1.94%. The fluid movement at the bottom of the well is mainly tangential flow, while the fluid in the slag discharge pipe is mainly axial flow. The construction parameters of efficient slag discharge are put forward: bit rotation speed is 8.7 r/min, gas injection rate is 4200 m^3/h, air duct sinking ratio is 0.84, and mud viscosity is 165 MPa·s. The research results can provide useful theoretical reference for large-scale sinking construction in deep wells.

Keywords Drilling shaft sinking · Gas lift reverse circulation · Multiphase coupling · Slag discharge flow field · Slag discharge effect

1 Introduction

With the sustained prosperity and development of China's economy, the total demand for coal consumption has increased year by year, the shallow coal resources in the central and eastern regions have been almost exhausted, and the focus of China's coal industry has shifted to the west. In recent years, a large number of large coal mines have been built in Xinjiang, Gansu, Inner Mongolia and Shaanxi (Cheng et al. 2023; Yao et al.2023; Fan, et al.2022; Liu et al.2021). The coal seam occurrence strata in mining areas in western China are mostly typical water-rich and weakly cemented rock strata, which are loose and easy to collapse, and the grouting sealing effect is poor, so it is difficult to construct vertical shaft by common law (Fan, et al.2022; Ji et al.2023; Yao et al.2022; Sun et al.2019; Fang et al.2022; Chen et al. 2020; Kang et al. 2023a, b). Drilling shaft sinking is a mechanized and automatic shaft sinking method that can cross deep and unstable strata. It has been successfully constructed in 79 vertical shafts in central and eastern China. Compared with freezing method, it has the advantages of high mechanization, good working environment and high quality of shaft wall (Cheng et al. 2023; Yao et al.2023; Liu et al. 2022; Yao et al.2019; Liu et al. 2015; Kang et al. 2023a, b). Recently, the Kekegai Coal Mine in the western mining area of Yanchang Petroleum, Shaanxi Province, adopted and successfully implemented the drilling method for the first time to construct the intake and return air shaft in the water-rich weakly cemented rock stratum, which proved the feasibility of the drilling method for the construction of the shaft in the western complex stratum (Cheng et al. 2023; Fan, et al.2022, 2023; Cui, et al.2022).

✉ Longhui Guo
guolonghui7864@163.com

1 School of Civil Engineering and Architecture, Anhui University of Science and Technology, Huainan, China

2 School of Resources and Environmental Engineering, Anhui University, Hefei, China

3 Anhui Provincial Key Laboratory of Building Structure and Underground Engineering, Anhui Jianzhu University, Hefei, China

4 China Coal Special Drilling Co.,Ltd., Hefei, China

However, in the process of drilling into Cretaceous-Jurassic argillaceous sandstone formation, there are engineering phenomena such as mud mutation, serious drilling tool wear and low drilling efficiency (Cheng et al. 2023; Liu et al.2021; Demirdag et al. 2014; Adebayo et al. 2014). Preliminary analysis shows that the distribution law of gas–liquid–solid coupling slag discharge flow field and the influencing factors of slag discharge effect are unclear, and the current design of slag suction port and well washing parameters cannot meet the requirements of efficient drilling in this kind of stratum, which is one of the main reasons leading to low drilling efficiency and needs to be studied and solved urgently.

Experts and scholars in related fields at home and abroad have carried out a lot of research on the optimization design of slag suction port, the distribution law of slag discharge flow field and the influencing factors of slag discharge effect, and achieved a series of results.

In the study of the optimization design of the bit slag suction port, the former Soviet Union conducted a field test to optimize the position and quantity of bit slag suction port when drilling in Donbass NO.27/35 mine. It was found that the loss of mud head of three slag suction ports was large, and the pumping speed of mud with single slag suction port was 1 ~ 2 times faster than that with three slag suction ports. The slag suction effect was better when the slag suction ports were arranged radially than circumferentially (Zhang et al. 2008). Wang et al. (2011) thinks that the slag suction port of large-diameter cone-bottom reaming bit should be arranged in the center of the bit, the slag suction port of truncated cone-bottom reaming bit should be arranged eccentrically, and the slag suction port should be designed as a rectangle with a length of about 1/3 of that of the leading bit. Huang et al. (2008) changed the chip removal groove of DTH bit from radial arrangement to tangential arrangement, which reduced the size and strength of vortex in bottom hole flow field and improved the chip removal ability. From the above, it can be seen that the layout of slag suction port of large-diameter vertical shaft drill bit is still stagnant in the exploration stage of the last century, and no systematic research method has been formed, and most of the existing research focuses on slag discharge of small-diameter drilling.

In the study of slag flow field distribution law, Huang et al. (2013), Hao et al. (2007) and Wang et al. (2007) studied the distribution law of gas–solid two-phase flow field in reverse circulation drilling of through-hole DTH hammer, and considered that the velocity, pressure, turbulence characteristics and rock-carrying capacity of gas phase in the flow field at the bottom of the hole were limited by the position where cuttings entered the flow field, particle diameter and hole bottom conditions. Jiao et al. (2020), Chen et al. 2020 and Meng et al. (2019) respectively simulated and analyzed the distribution law of the flow field of air, foam and fluid washing and slag discharge in large-diameter shaft boring machine, and studied the influence of the clearance height at the bottom of the well, the diameter of slag discharge pipe, the diameter, number and angle of jet orifices on the velocity and pressure distribution of the flow field at the bottom of the well. Large-diameter shaft drilling rig is different from DTH hammer and shaft boring machine in construction technology, slag discharge mode, drilling diameter and well washing medium, and its slag discharge flow field is also quite different.

In the study of the influencing factors of slag discharge effect, Wang et al. (2020), Fan et al. (2020) and Qu et al. (2021) studied the liquid–solid two-phase coupling slag discharge in oil and gas wells, and considered that the main factors affecting the migration of drilling debris are: the displacement of well washing fluid, the hole size, the angle of inclination, the particle size and density of cuttings, the density and viscosity of well washing fluid, the rotation speed of drill pipe, etc. Ozbayoglu et al. (2005), Kamyab et al. (2016), Oseh et al. (2020) and Vaziri et al. (2020) studied the transportation of cuttings when drilling horizontal oil and gas wells, and thought that the drilling fluid with high flow rate and low viscosity has stronger ability to transport cuttings horizontally, and increasing the flushing volume of drilling fluid and the mechanical rotation speed of drilling tools can effectively improve the transportation efficiency of cuttings. Liu et al. (2013), Zhou et al. (2018) and Xiong et al. (2014) respectively studied the slag discharge parameters of reverse circulation drilling for anchor holes in roadway floor, bored piles and gas pumping wells, and considered that the main factors affecting the slag discharge effect were drilling depth, particle size of drilling slag, mud circulation, gas injection rate and gas injection pressure, and put forward a reasonable combination of slag discharge parameters. Most of the above research focuses on small-sized oil and gas wells, gas surface pumping wells, cast-in-place pile holes and anchor holes in roadway floor, and their drilling size, slag discharge flow pattern and motion characteristics are different from those of large-diameter vertical shaft drilling.

In summary, this paper takes the φ4.2 m advanced drilling of the central return air shaft in Kekegai Coal Mine in the western mining area as the research background, adopts the method of combining CFD-DEM with similar model tests, establishes the numerical model of gas–liquid–solid multiphase coupling slag discharge and the visual slag discharge test platform respectively, optimizes the layout of the slag suction port of the shaft sinking drill in large-diameter coal mine, studies the distribution law of liquid–solid–gas multiphase coupling slag discharge flow field and the influencing factors of slag discharge effect, and puts forward the technical parameters and optimization countermeasures of efficient well washing slag discharge.

Fig. 1 AD130/1000 shaft drilling rig

2 Engineering background

Kekegai Coal Mine is located in Yulin City, Shaanxi Province, with a designed production capacity of 10 Mt/a (Fig. 1). The coal seam occurrence stratum is a typical water-rich and weakly cemented rock stratum in the west, and its central intake and return vertical shaft is the first vertical shaft constructed by drilling method in the west of China (Cheng et al. 2023; Yao et al.2022). The design depth of the central return air shaft is 521.5 m, the net diameter is 6 m, the thickness of the shaft wall is 600 mm, and the drilling diameter is 8.5 m. The AD130/1000 full hydraulic power shaft drilling rig was used for two-stage drilling, including φ4.2 m advanced drilling and φ8.5 m reaming drilling, in which the advanced drilling used a flat-bottomed hob bit with a diameter of 4.2 m, and the well washing method used a gas-lift reverse circulation mud suspension slag removal process. The construction process of drilling method for central return air shaft in Kekegai Mine is shown in Fig. 2.

3 Numerical model establishment

3.1 Mathematical control equation

Gas lift reverse circulation slag removal is a three-phase coupling movement process of mud, rock slag and compressed air. The Euler multiphase flow model and Standard $k-\varepsilon$

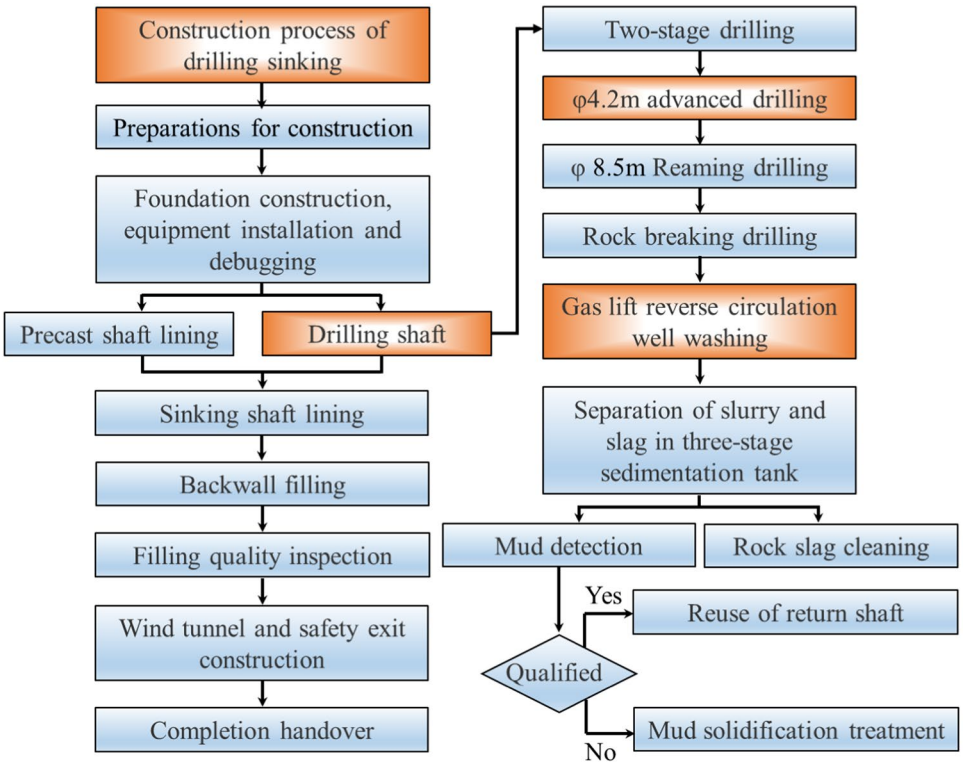

Fig. 2 Construction process of central return air shaft drilling method in Kekegai Mine

turbulence model are selected to calculate the movement and distribution of mud and air in the slag removal flow field, and the continuity equation and momentum conservation equation of fluid phase are established in Euler coordinate system (Yan et al.2020; Akhshik et al. 2016a, b), which are as follows:

$$\frac{\partial}{\partial t}(\alpha_i\rho_i)+\nabla\cdot(\alpha_i\rho_i v_i)=0 \tag{1}$$

$$\frac{\partial}{\partial t}(\alpha_i\rho_i v_i)+\nabla\cdot(\alpha_i\rho_i v_i v_i)=-\alpha_i\nabla P+\nabla\cdot\tau_i+\alpha_i\rho_i g+F_i \tag{2}$$

where i is liquid or gas phase; α_i is volume fraction of i phase; ρ_i is density of i phase, kg/m^3; v_i is velocity of i phase, m/s; P is the interphase pressure, MPa; τ_i is stress–strain tensor of i phase; F_i is the interaction between rock slag and fluid, N; g is the acceleration of gravity, m/s^2.

The discrete element simulation software EDEM is selected to calculate the movement and distribution of rock slag in the slag discharge flow field, and the collision and extrusion between rock slag were simulated by Hertz-Mindlin non-slip elastic contact model, and the movement of rock slag satisfies Newton's second law (Shao et al.2020; Akhshik et al. 2016a, b).

$$m_s\frac{dv_s}{dt}=mg(1-\frac{\rho_l}{\rho_s})+F_f+F_c \tag{3}$$

where m_s is the quality of rock slag, kg; v_s is the velocity of rock slag, m/s; ρ_s is the density of rock slag, kg/m^3; ρ_l is the density of mud, kg/m^3; F_f is Newton's resistance to cuttings, N; F_c is the resultant force of cuttings contacting with other cuttings and walls, N.

The conservation equation of angular momentum of rock slag particles is:

$$\frac{d}{dt}(Iw_s)=T_a+T_r+T_t \tag{4}$$

where I is the moment of inertia of rock slag, kg m^2; w_s is angular velocity, rad/s; T_a, T_r, T_t are the axial, radial and tangential torques of rock slag, N m.

3.2 Numerical model

Combined with the construction technology of gas-lift reverse circulation slag discharge and the structural form, slag suction port arrangement and cutter arrangement of φ4.2 m advanced drill bit in the central return air shaft of Cocoa Cover, a scaled numerical model of gas-lift reverse circulation slag discharge was established by CFD-DEM research method (1/12 of the prototype). The model mainly includes bottom hole, slag discharge pipe and drill bit, in which the bottom hole and slag discharge pipe are set as fluid domain, and the drill bit is set as rotation domain, and the model is divided by tetrahedral grid, as shown in Fig. 3.

The numerical model is solved in the fluid simulation software Fluent and the discrete element simulation software EDEM respectively. The calculation flow is shown in Fig. 4 and the model parameters are shown in Table 1.

4 Optimization of slag suction port of bit and distribution law of slag discharge flow field

4.1 Optimization content and evaluation index

As shown in Fig. 5, by adjusting the number, spacing, area ratio and total area of the slag suction port, the numerical models with the number of slag suction ports of 1, 2 and 3, the length-diameter ratio α (the ratio of the spacing of the slag suction port to the radius of the drill bit) of 0.3, 0.4 and 0.5, the area ratio β (the ratio of the area of the two slag suction ports) of 1, 0.5, 0.25 and 0.17, and the total area ratio γ (the percentage of the ratio of the total area of the slag suction port to the cross-sectional area of the drill bit) of 1.63%, 1.78%, 1.94% and 2.12%, respectively, are established in turn. Taking the slag removal rate η, mud transport ratio λ and pneumatic conveying ratio ξ as evaluation indexes, the layout of each group of slag suction ports is optimized, and other influencing factors are changed based on the optimization results, and the best layout of slag suction ports is finally selected by step optimization.

$$\begin{cases}\eta=\dfrac{\sum M_s}{\sum M_{total}}\\ \lambda=\dfrac{\sum M_s}{\sum M_l}\\ \xi=\dfrac{\sum M_s}{\sum M_g}\end{cases} \tag{5}$$

where M_{total}, M_s, M_l and M_g are respectively the quality of generated rock slag, the quality of discharged rock slag, the quality of discharged mud and the quality of input gas.

4.2 Optimization result

As shown in Fig. 6, when the area of the cutter head slag suction port is the same, the slag removal effect of the double slag suction port arrangement is the best, and the slag removal rate is increased by 76.5% and 14.2% respectively compared with that of the single slag suction port and three slag suction ports model, and the mud carrying capacity and pneumatic lifting capacity are also significantly enhanced.

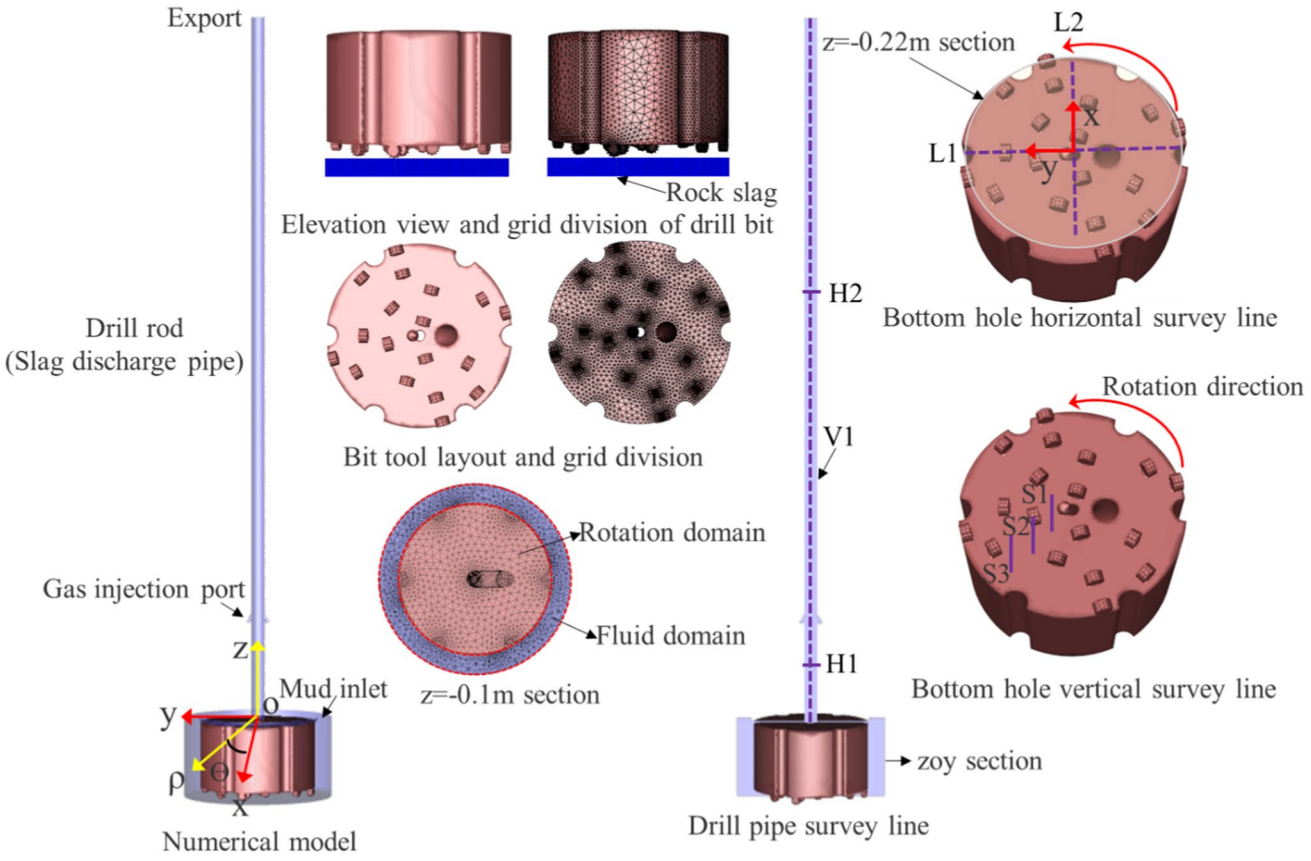

Fig. 3 Numerical model of slag discharge and layout of survey line

There is an optimal threshold value for the distance between the two slag suction ports, not as close as possible or as far as possible, and the slag removal effect is the best when the length-diameter ratio is 0.4, and the slag removal rate increases by 19.7% and 92.2% for the numerical models with the length-diameter ratio of 0.3 and 0.5 respectively. Each slag discharge index increases with the increase of the area ratio of slag suction port, and the area ratio of slag suction port is preferably 1. The slag removal rate of this model is 64.3% higher than that of the field model of slag suction port. With the continuous increase of the area of the slag suction port, all the slag discharge indexes show a slight increase and then decrease. It can be seen that excessive increase of the area of the slag suction port will reduce the slag discharge effect, so the proportion of the total area γ of the slag suction port is preferably 1.94, and the slag removal rate is increased by 66.06% compared with the on-site double slag suction port arrangement.

4.3 Distribution law of slag discharge flow field

As shown in Fig. 3, a vertical survey line V1 is set at $y=0$ m of the slag discharge pipe in the zoy section of the numerical model, and two horizontal survey lines H1 and H2 are set at $z=0.2$ m and $z=1.5$ m respectively. Two horizontal survey lines L1 and L2 are set in the cross section of $z=-0.22$ m at the bottom of the well, and three vertical survey lines S1 to S3 are set radially at the bottom of the well. The above survey lines are used to monitor the velocity and pressure of fluid in the slag discharge pipe and the bottom hole, and then compare and analyze the distribution law of slag discharge flow field between the field model and the optimized model.

4.3.1 Flow field in slag discharge pipe

The velocity and pressure distribution in the slag discharge pipe of the field model and the optimized model are shown in Fig. 7.

From the analysis of Fig. 7a and b, it can be seen that the movement path of mud carrying rock in the slag discharge pipe can be divided into liquid–solid section and liquid–solid–gas section according to the manifold. When passing through the gas injection end, the manifold of mixed fluid changes, the density and pressure suddenly decrease, and the pressure in the optimized model pipe is lower than that in the field model. Therefore, under the pressure difference of the mud column outside the pipe and the gas lift of compressed air inside the pipe, the axial velocities of mud

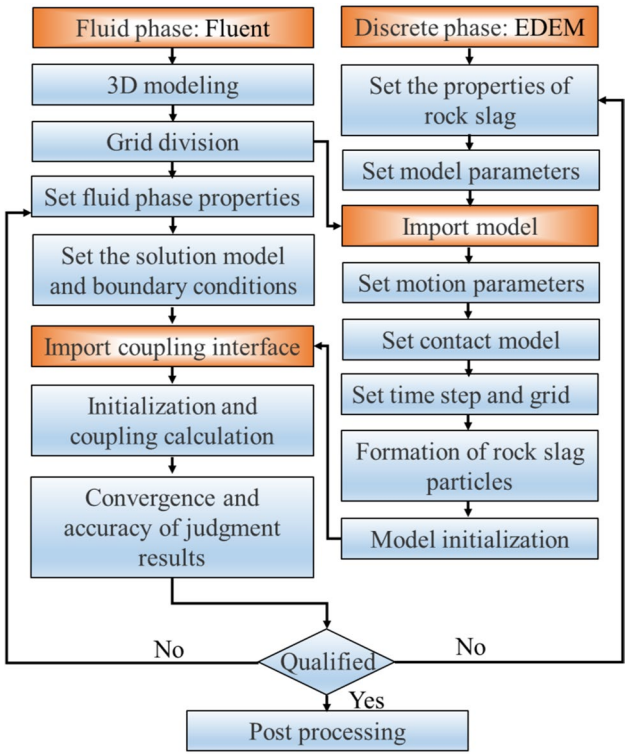

Fig. 4 Numerical model calculation process

Table 1 Selection of modeling parameters

Parameter	Symbol	Unit	Value
Cutter head speed	w	r/min	30
Mud density	ρ_l	kg/m^3	1100
Gas injection density	ρ_g	kg/m^3	1.29
Rock slag density	ρ_s	kg/m^3	2350
Cutter head diameter	D_1	m	0.35
Duct diameter	d_1	m	5.4×10^{-3}
Buried depth of air duct	L_1	m	1.8
Rock slag diameter	d_s	m	3×10^{-3}
Drill pipe diameter	d_2	m	4×10^{-2}
Drill pipe length	L_2	m	2.15
Shaft diameter	D_2	m	0.45
Mud viscosity	μ_l	mPa·s	8
Gas injection flow rate	Q_g	m^3/h	8.4
Bottom hole pressure	P_1	MPa	3×10^{-3}

and rock slag are greatly increased. The mud and rock slag of the field model are increased by 86% and 111% respectively, and the mud and rock slag of the optimized model are increased by 82% and 91% respectively. The average upward velocity of mud and rock slag in the slag discharge pipe of the optimized model increased by 2.2% and 4.2% respectively compared with the field model.

From the analysis of Figs. 7c and d, it can be seen that along the section of the slag discharge pipe, the high-speed mud flow is mainly distributed in the central area of the slag discharge pipe (accounting for about 70% of the section of the slag discharge pipe), and near the wall, the mud flow speed is rapidly reduced due to viscous resistance; The change of fluid flow pressure in the slag discharge pipe reflects the change of kinetic energy. The kinetic energy distribution of the two horizontal lines in the pipe is parabolic, and the kinetic energy at the center is the largest and gradually decreases to both sides. The flow pressure of the upper and lower lines at the gas injection end of the optimized model is increased by 7% and 16% respectively compared with the field model.

4.3.2 Bottom hole flow field

The velocity and pressure distribution of bottom hole fluid in the field model and the optimized model are shown in Figs. 8 and 9.

As can be seen from the analysis of Fig. 8, The axial movement of bottom hole fluid is mainly concentrated near the slag suction port. In the field model, the adsorption capacity of the swept slag suction port is stronger than that of the central slag suction port, and the axial velocity of the fluid at the slag suction port is increased by 35.4% compared with that of the central slag suction port. The upward velocity of the bottom hole fluid in the optimized model is greatly improved compared with that in the field model. The optimized model maintains the adsorption capacity of the original site model to sweep the slag suction port, and improves the shortcomings of the site model, such as insufficient adsorption capacity of the central slag suction port and small adsorption area, which makes the upward velocity of bottom hole mud increase by 118.3% and the diameter of adsorption area increase by 20.3%.

The horizontal velocity of bottomhole fluid is much larger than the axial velocity, and the horizontal flow is mainly tangential. Taking the optimized model L1 survey line as an example, its average tangential velocity is about 16.7 times of the axial velocity and 2.3 times of the radial velocity. Compared with the field model, the average axial velocity, radial velocity and tangential velocity of bottomhole fluid in the optimized model increase by 18.9%, 6.1% and 30.9% respectively. The radial movement of bottom hole fluid is obvious only near the slag suction port, and far away from the slag suction port, the radial velocity of mud is small, the scouring ability of rock slag is weak, and the centrifugal effect and pressure holding effect of rock slag are serious, so it is easy to accumulate cuttings (Xia et al.2013).

The distribution of bottom hole pressure decreases approximately linearly from outside to inside along the radial direction, while the pressure difference of bottom

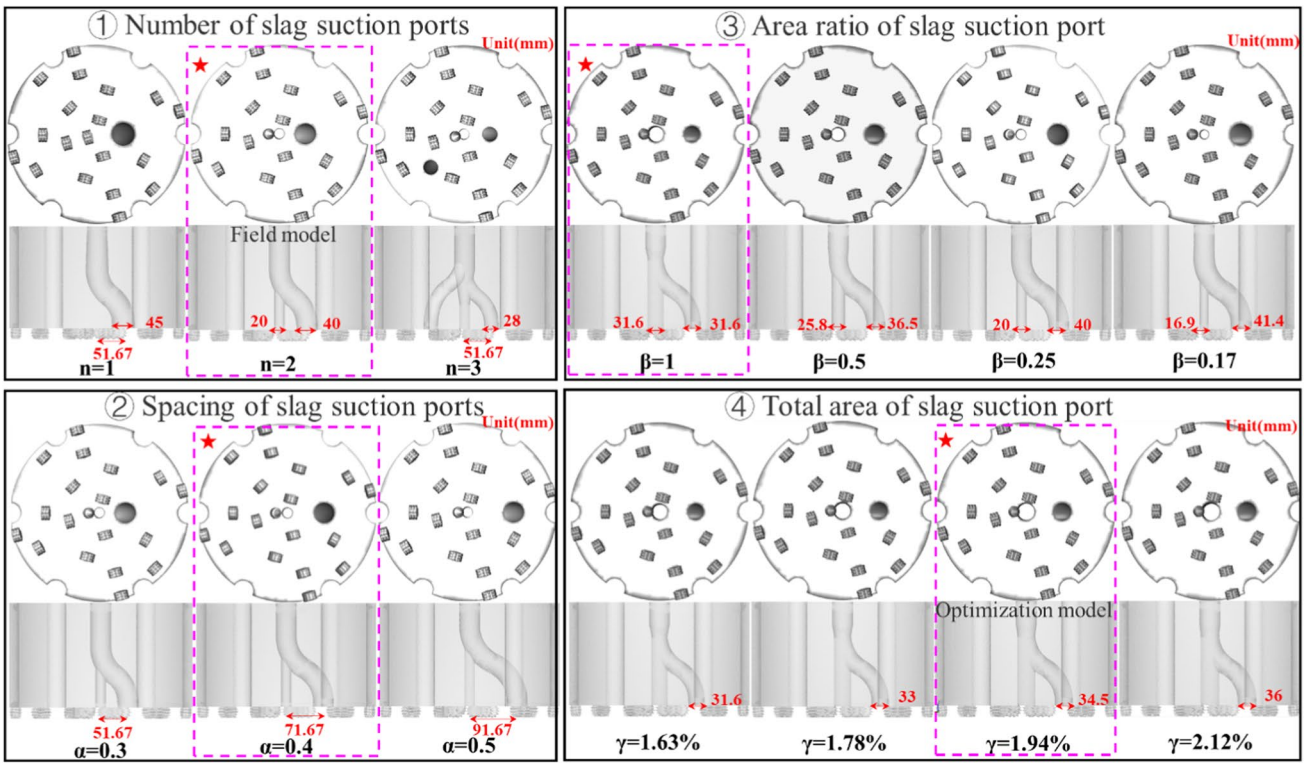

Fig. 5 Numerical model of slag suction port arrangement under different factors

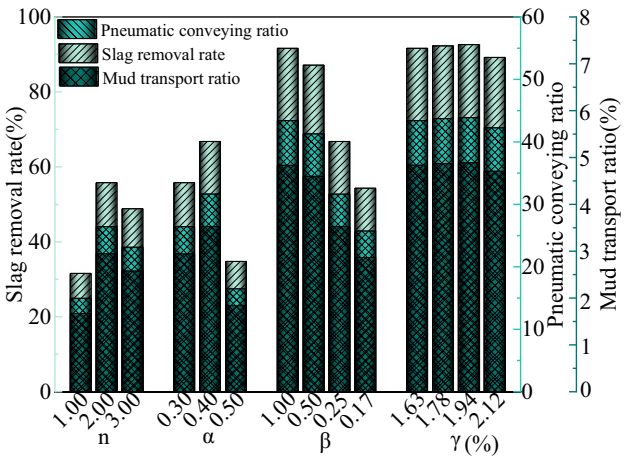

Fig. 6 Optimization results of slag suction port

hole fluid increases approximately linearly from outside to inside along the radial direction. The bottom hole pressure of the field model and the optimized model decreases to the lowest at the swept slag suction port and the central slag suction port respectively, and the bottom hole pressure of the optimized model is smaller than that of the field model, so the greater the pressure difference of bottom hole fluid in the optimized model, the more easily the bottom hole mud and rock slag are adsorbed and lifted.

As can be seen from the analysis of Fig. 9, The fluid movement in the vertical direction of the bottom hole clearance is mainly tangential flow. Taking the linear velocity distribution of the optimized model S1 as an example, the average tangential velocity is about 21 times and 6 times of the axial and radial velocity respectively, and the axial, radial and tangential velocities of the optimized model are increased by 43.8%, 48.2% and 17.6% respectively compared with the field model.

The fluid on the surface of the drill bit and the rock-breaking surface hardly moves axially and radially, but its axial and radial velocities reach the peak at the clearance center of the bottom hole and 5 mm above the rock-breaking surface, respectively. Due to the adsorption of the slag suction port, the axial and radial velocities of the fluid increase closer to the slag suction port (Such as S1 survey line), while the mud hardly moves axially and the radial velocity decreases greatly away from the slag suction port (Such as S3 survey line).

The tangential movement of the clearance fluid at the bottom of the well can be divided into three sections in the vertical direction. First, near the surface of the drill bit (20 ~ 25 mm away from the bottom of the well), the mud flow rotates in the same direction with the drill bit, and its

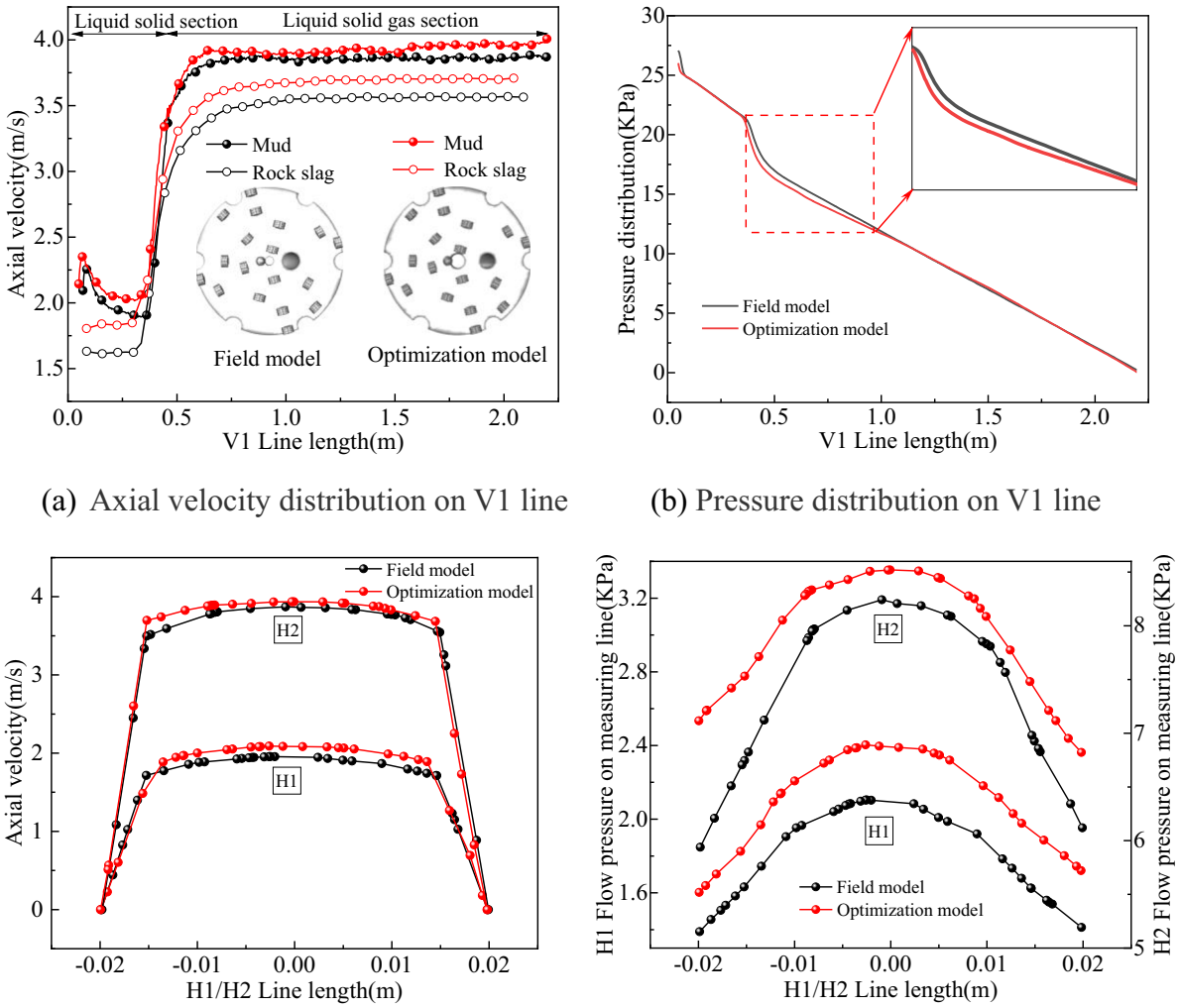

(a) Axial velocity distribution on V1 line

(b) Pressure distribution on V1 line

(c)Axial velocity distribution on H1 and H2 lines

(d) Distribution of flow pressure on H1 and H2 Lines

Fig. 7 Distribution law of flow field in slag discharge pipe

circulation degree increases with the increase of the radius of the drill bit. Secondly, in the range of 8 ~ 20 mm away from the bottom of the well, the drag effect of the drill bit on the mud is equal to its viscous resistance, and the mud moves tangentially at a constant speed, and the tangential speed increases with the decrease of the radius of the drill bit. Thirdly, within the range of 8 mm from the bottom hole, the viscosity of mud plays a leading role, and its circulation speed decreases with the decrease of the distance from the bottom hole until it is 0.

4.3.3 Migration law of rock slag

The field model and the optimized model are selected to analyze the distribution state of rock slag at the bottom of the well and in the slag discharge pipe at different times, and their migration laws such as convergence, suspension, adsorption and lifting are analyzed.

As can be seen from the analysis of Fig. 10, the rock slag moves along the bottom of the well in a dynamic cycle of "convergence-suspension-adsorption-lifting". The rock slag is transported by mud and lifted by pneumatic force in the slag discharge pipe, and the mixed fluid successively returns at high speed in liquid–solid and liquid–solid–gas state until it is discharged from the ground. During the whole slag discharge process, the rock slag moves circularly until the rock slag at the bottom of the well is dynamically cleared.

In the vicinity of the slag suction port, the adsorption force of the slag suction port plays a leading role, and the mud carries the slag in the same direction with the drill

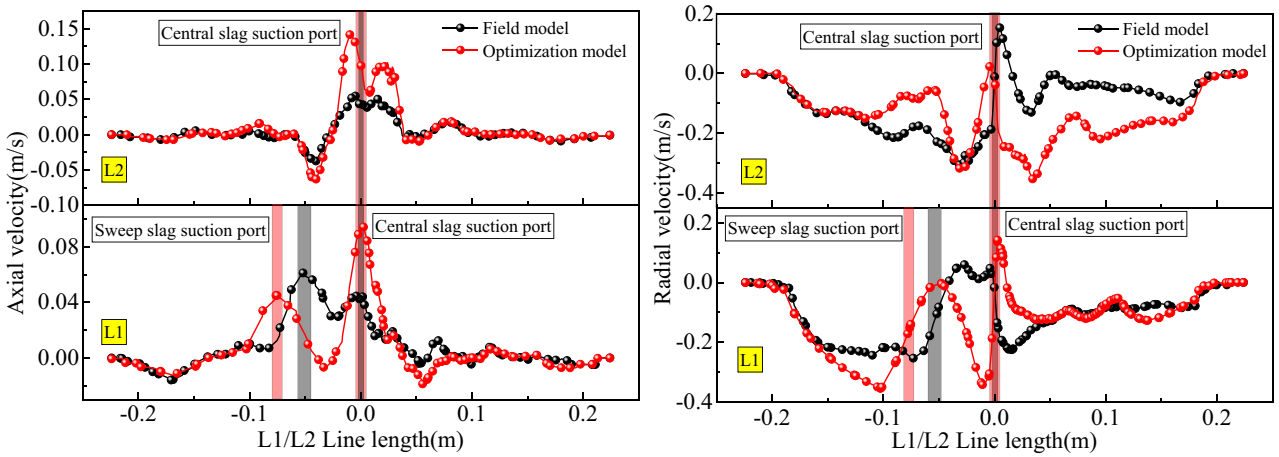

(a) Axial velocity distribution on L1 and L2 lines (b) Radial velocity distribution on L1 and L2 lines

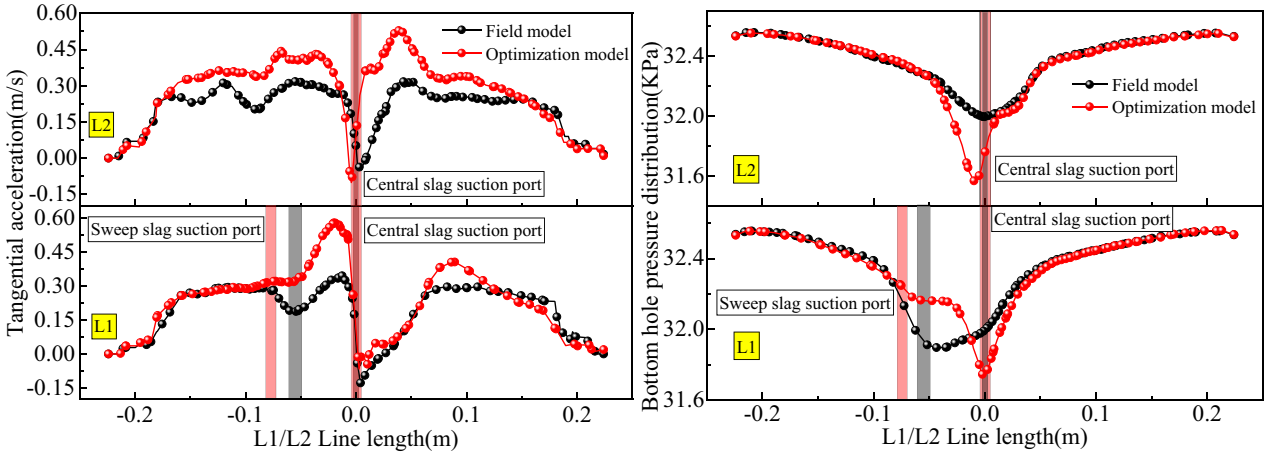

(c)Tangential velocity distribution on L1 and L2 lines (d) Pressure distribution on L1 and L2 lines

Fig. 8 Distribution law of flow field on bottom hole horizontal measuring line

bit and moves spirally to the slag suction port. Far away from the slag suction port, the radial velocity of the slag is small and centrifugal movement is easy to occur. In this area, the mud pressure holding effect is serious, and the rock slag is easily thrown out of the outside of the drill bit, so it is easy to accumulate cuttings.

The optimized model has improved the current situation of insufficient aggregation ability and poor suspension degree of rock slag at the bottom of the well, and the upward velocity, density distribution and lifting effect of rock slag in the slag discharge pipe have also been significantly improved, and the slag discharge efficiency has been greatly improved.

5 Model test study on slag discharge effect and its influencing factors

In order to study the slag removal effect of gas lift reverse circulation and its influencing factors, a set of experimental device simulating gas-lift reverse circulation slag discharge was developed, and the similar model test of gas-lift reverse circulation slag discharge was carried out.

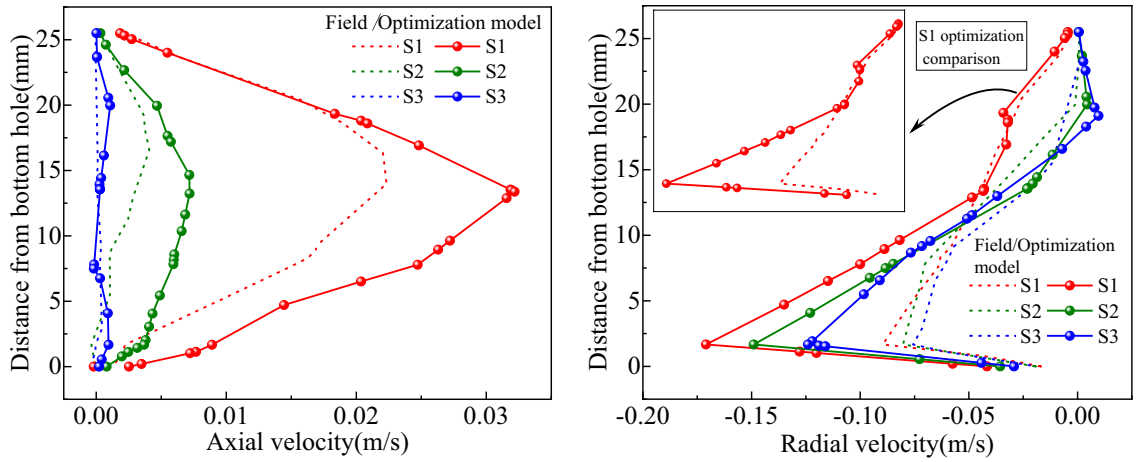

(a) Axial velocity distribution on S1~S3 survey line (b) Radial velocity distribution on S1~S3 survey line

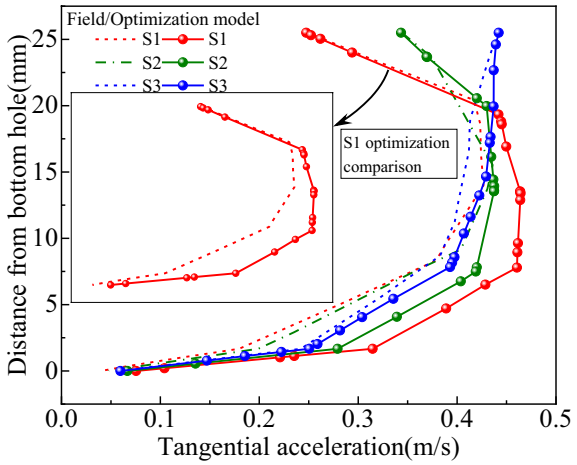

(c)Tangential velocity distribution on S1~S3 survey line

Fig. 9 Distribution law of flow field on radial vertical survey line at bottom hole

5.1 Similar model design

Based on the similarity theory and dimensional analysis method, the similarity criterion of the gas lift reverse circulation slag discharge test system is derived. Considering the construction characteristics and test conditions of the drilling method, Determine geometric similarity constant $\lambda_l = 12$, density similarity constant $\lambda_\rho = 1$, motion similarity constant $\lambda_v = 2\sqrt{3}$, cutter head speed similarity constant $\lambda_w = 1/2\sqrt{3}$, gas injection flow similarity constant $\lambda_{Qg} = 500$, mud viscosity similarity constant $\lambda_\mu = 30$, stress similarity constant $\lambda_\sigma = 12$ and time similarity constant $\lambda_t = 2\sqrt{3}$.

According to the above similar conditions and the characteristics of drilling sinking construction, some parameters of model test are determined, as shown in Table 2.

5.2 Test equipment

In order to realize the visual study of multiphase flow of gas lift reverse circulation slag discharge, combined with the similarity criterion and the construction conditions of drilling method, a set of test device for simulating gas lift reverse circulation slurry suspension slag discharge was developed. The device is mainly composed of test stand, test cavity, drill bit, drill pipe and other parts (Cheng et al. 2023).

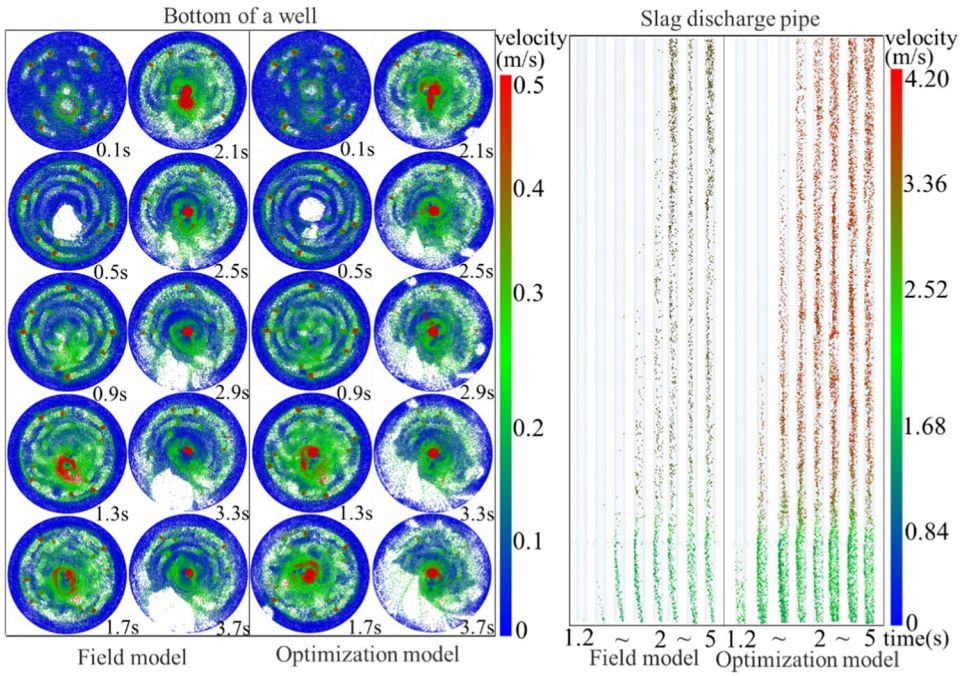

Fig. 10 Field model and optimization model bottom hole and slag discharge pipe rock slag distribution

Table 2 Selection of model test parameters

Parameter type	Parameter	Symbol	Unit	Prototype value	Model value
Drilling parameters	Cutter head rotation speed	w	r/min	5 ~ 10	17 ~ 35
	Cutter head drilling speed	v	mm/min	4 ~ 11.5	1.2 ~ 3.3
	Cutter head diameter	D_1	m	4.2	0.35
Gas injection parameters	Gas density	ρ_g	kg/m^3	1.29	1.29
	Gas injection flow rate	Q_g	m^3/h	3600 ~ 4800	7.2 ~ 9.6
	Gas injection pressure	P_g	MPa	1.8	0.15
	Duct diameter	d_1	m	95×10^{-2}	8×10^{-3}
	Buried depth of air duct	L_1	m	-	1.8
Mud parameters	Mud density	ρ_l	kg/m^3	1045 ~ 1288	1100
	Mud viscosity	μ_l	mPa·s	90 ~ 240	3 ~ 8
Rock slag parameters	Rock slag density	ρ_s	kg/m^3	2000 ~ 2600	2350
	Rock slag diameter	d_s	m	$3 \sim 50 \times 10^{-3}$	$1 \sim 4 \times 10^{-3}$
	Tensile strength	P_s	MPa	0.8 ~ 1.2	0.06 ~ 0.1
Drill pipe parameters	Drill pipe length	L_2	m	-	2.15
	Drill pipe diameter	d_2	m	0.48	4×10^{-2}
Other parameters	Well cleaning time	t	s	630	180
	Shaft diameter	D_2	m	6	0.45

The test stand is 0.75 m long, 0.75 m wide and 2.75 m high. Both the test cavity and the drill pipe are made of transparent acrylic material. The test chamber has a diameter of 0.45 m and a height of 2 m, and both drilling and slag discharge are completed in it. The drill pipe is 4 cm in diameter and 2.15 m in length. The upper part is connected to the engine and the lower part is connected to the drill bit. The structure of the drill bit, hob arrangement and slag suction port arrangement are consistent with the field model and optimization model in Fig. 5 in Sect. 4.1. The rotation speed and drilling speed of the drill bit can be adjusted by adjusting the governor and the lifting speed of the oil cylinder respectively. One end of the air hose is inserted into the drill pipe, and the other end is connected to the air compressor. The gas injection pressure and gas injection flow are adjusted by the pressure regulating valve and the gas flowmeter (Fig. 11). After the rock slag and mud are discharged, they are separated by the filter screen, the separated mud is weighed and recorded, the rock slag is dried and screened, and its quality and particle gradation are recorded. During

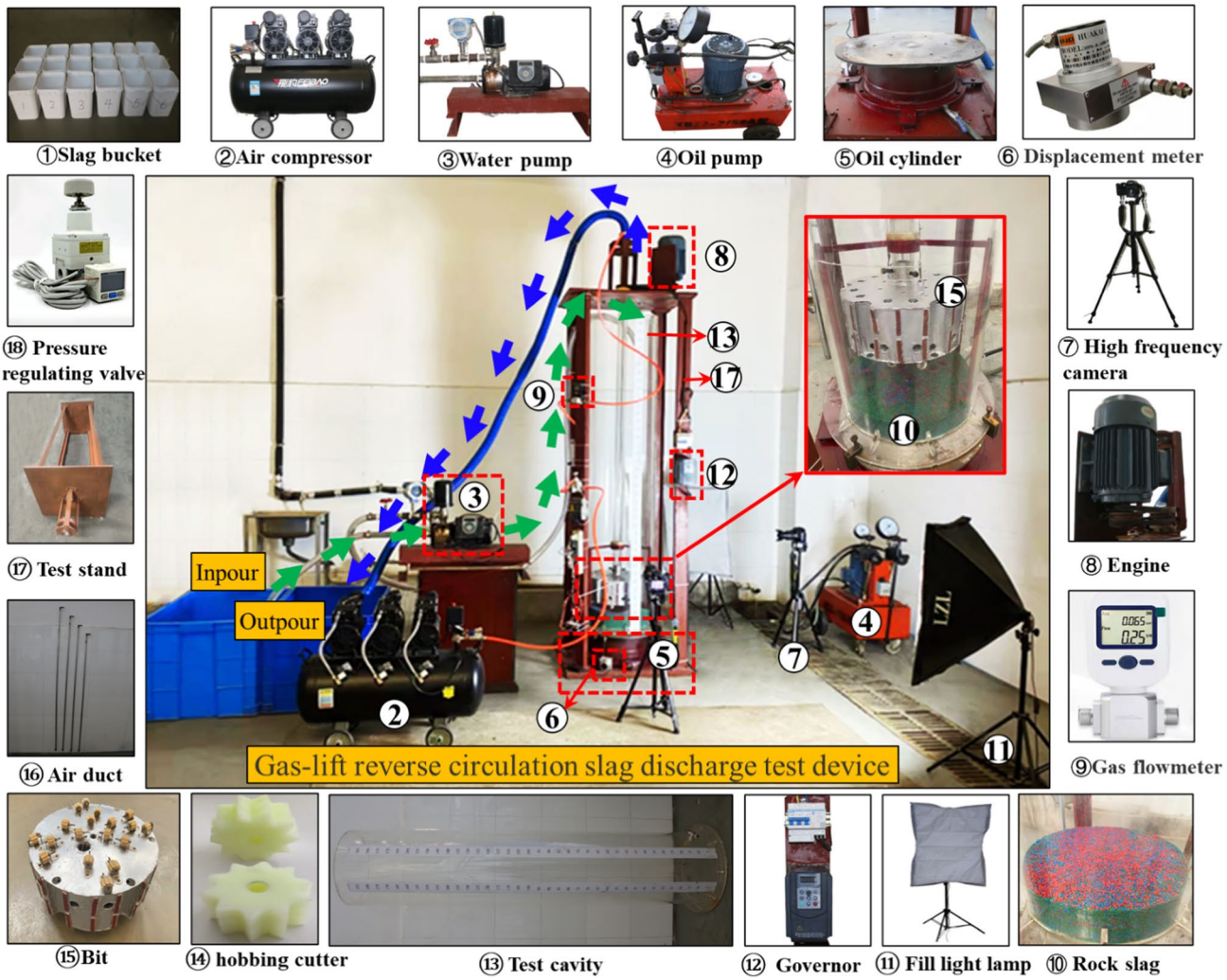

Fig. 11 Gas lift reverse circulation slag discharge test device and some components

the experiment, the replenishment slurry was continuously pumped into the test cavity by the water pump to ensure the normal circulation of the slurry, and the movement characteristics of the rock slag were recorded by the high frequency camera. The operation process and method of the test device are shown in Reference (Cheng et al. 2023).

5.3 Similar material

5.3.1 Mud similar material

The density distribution of mud in Kekegai Coal Mine is stable, but the mud viscosity distribution is quite different. Therefore, the mud similar materials are prepared with viscosity as the main index.

Mud samples were taken from several strata in the field and their laboratory average viscosities were measured, which were converted into target viscosities according to similar conditions. Finally, sodium chloride was selected as the weighting agent and mud powder as the tackifier, and a "transparent" mud similar material with five horizontal gradients of density of 1.1 g/cm^3 and viscosity of 1 mPa·s (water), 1.7 mPa·s, 5.5 mPa·s, 8.2 mPa·s and 11 mPa·s was prepared according to the proportion in Fig. 12.

5.3.2 Rock slag similar material

According to the density, particle size, tensile strength and similarity criteria of the rock slag in the Cretaceous-Jurassic strata, colored glass balls with particle sizes of 1 mm to 2 mm, 2 mm to 3 mm and 3 mm to 4 mm are selected to simulate the rock slag (Xu et al.2024; Liu et al.2024). The mixing density of rock slag similar materials is 2350 kg/m^3, and the weak cementation is simulated by bonding glass balls with super glue. The glass balls are prominent in color, easy to catch, pollution-free and reusable (Fig. 13).

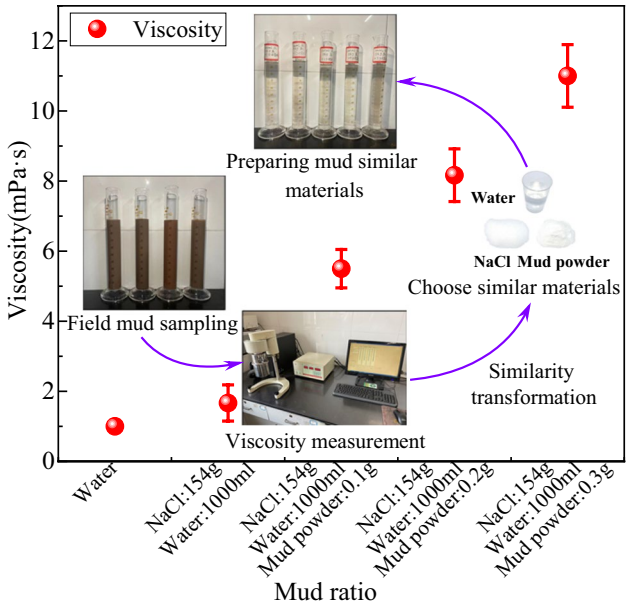

Fig. 12 Proportion and preparation process of mud similar material

5.4 Analysis of influencing factors of slag discharge effect

5.4.1 Bit rotation speed

The slag discharge effect when the bit rotation speed is 20–40 r/min is shown in Fig. 14.

As can be seen from the analysis of Fig. 14a, the displacement of rock slag first increases and then decreases with the increase of bit rotation speed, and the displacement of mud decreases slightly with the increase of bit rotation speed. Moreover, the displacement of rock slag and mud in the optimized model is significantly higher than that in the field model. When the drill bit rotation speed is increased from 20 to 30 r/min, the rock slag displacement of the optimized model is increased from 0.94 kg to 1.61 kg, with an increase rate of 71.28%. When the drill bit rotation speed is greater than 30r/min, the rock slag displacement is slightly reduced. When the bit rotation speed is increased from 20 to 40 r/min, the mud displacement is reduced from 141.38 kg to 130.58 kg, with a reduction rate of 7.64%. The displacement of rock slag and mud in the optimized model increased by 11.59% and 2.00% respectively compared with the field model. This is because when the bit speed increases, it will increase the disturbance to the rock slag and the adsorption path of the slag suction port will also increase exponentially, effectively increasing the adsorption efficiency of the slag suction port. However, when the rotating speed exceeds a certain threshold, the centrifugal force of the mud flow and the rock slag will gradually increase, and part of the rock slag will be thrown to the outer edge of the drill bit, and the rotating mud flow will have a certain blocking effect on the replenishment mud and the circulating flow of the mud, Therefore, with the increase of bit speed, the displacement of rock slag first increases and then decreases, and the displacement of mud decreases slightly.

As can be seen from the analysis of Fig. 14b, slag discharge efficiency, mud transport ratio and pneumatic conveying ratio all increase at first and then decrease with the increase of bit rotation speed. When the bit speed is 30 r/min, the slag discharge efficiency of the optimized model is 71.02% higher than that of the low speed of 20 r/min and 17.7% higher than that of the high speed of 40 r/min, and the slag discharge efficiency of the optimized model is 21.89% higher than that of the field model. Therefore, when the bit speed is 30 r/min, it can not only meet the suspension degree of rock slag, balance the adsorption

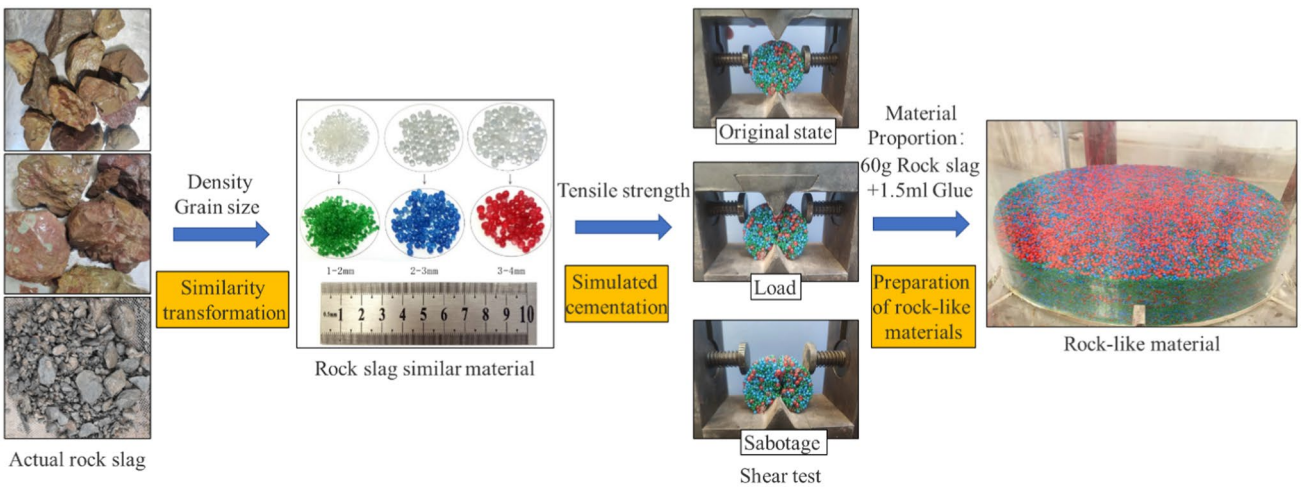

Fig. 13 Preparation process of rock slag similar materials

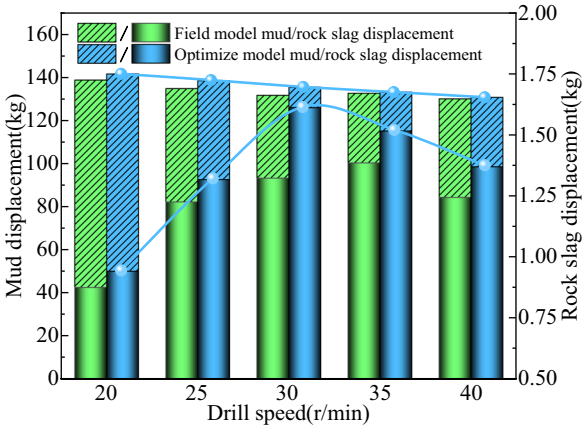

(a) Displacement of rock slag and mud

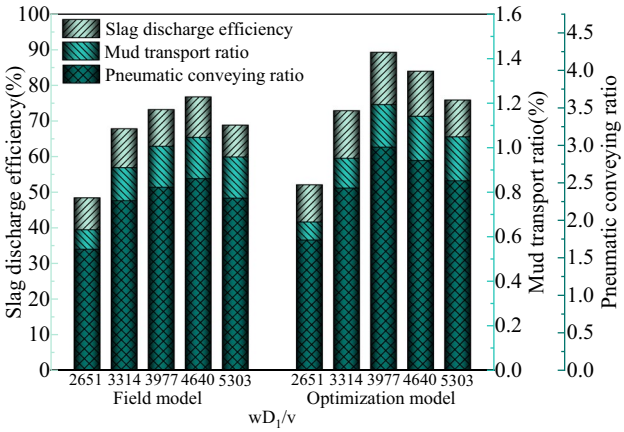

(b) Trend chart of slag discharge index

Fig. 14 Influence of bit rotation speed on slag discharge effect of field model and optimized model

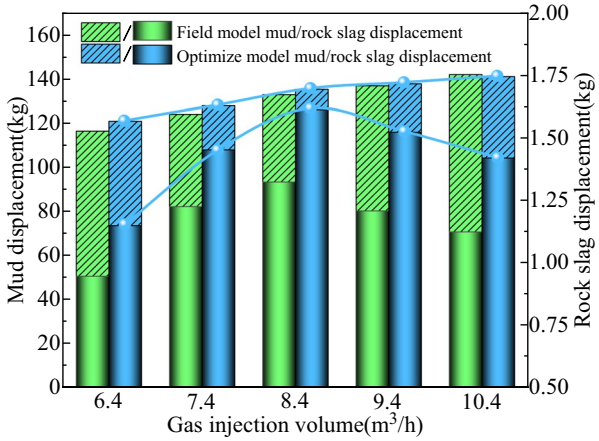

(a) Displacement of rock slag and mud

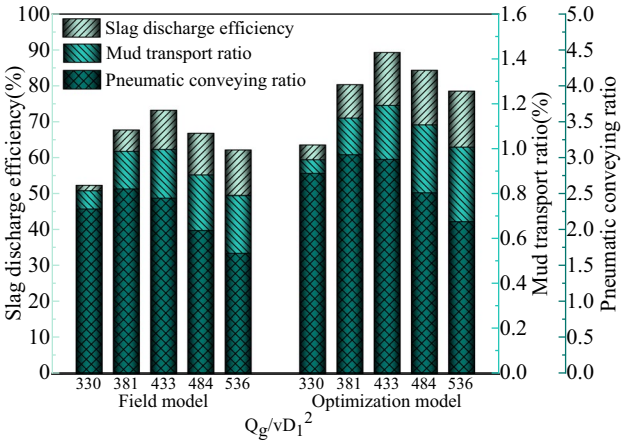

(b) Trend chart of slag discharge index

Fig. 15 Influence of gas injection volume on slag discharge effect of field model and optimized model

force and centrifugal force, but also realize efficient slag discharge, which is energy-saving and economical.

5.4.2 Gas injection volume

The slag discharge effect when the gas injection volume is 6.4–10.4 m^3/h is shown in Fig. 15.

As can be seen from the analysis of Fig. 15a, increasing the gas injection volume can greatly increase the displacement of mud, and the displacement of rock slag first increases and then decreases with the increase of gas injection volume, and the displacement of mud and rock slag in the optimized model is the largest. When the gas injection volume is increased from 6.4 m^3/h to 10.4 m^3/h, the mud displacement of the optimized model is increased from 120.78 kg to 140.91 kg, achieving an increase of 16.67%, while the rock slag displacement is greatly increased by 40% at first, and then slightly decreased by 13.38%, and the average mud and rock residue displacement are increased by 2.00% and 22.85% respectively compared with the field model. This is because increasing the gas injection means increasing the input energy of the gas-lift reverse circulation slag removal system, and the kinetic energy obtained by the three-phase flow of mud-rock slag- air also increases, and the rock carrying capacity and pneumatic lifting capacity of mud are enhanced. On the other hand, the gas phase content in the slag discharge pipe increases, the density of mixed fluid decreases, the pressure difference between the inside and outside of the slag discharge pipe increases, and the mixed fluid is easy to obtain high flow rate, so the displacement of mud and rock slag is significantly improved. However, when the gas injection volume exceeds a certain critical value, the friction between the three-phase fluid and the inner wall of the slag discharge pipe increases, which intensifies the pressure loss in the slag discharge pipe and the well wall

annulus, and the volume fraction of rock-carrying carrier mud in the slag discharge pipe decreases sharply, which weakens the rock-carrying capacity. Therefore, excessive gas injection volume will lead to a slight decrease in the rock slag displacement.

As can be seen from the analysis of Fig. 15b, With the increase of gas injection volume, all slag discharge indexes increase first and then decrease, and the influence on pneumatic conveying ratio is the most significant. Among the two indicators of slag discharge efficiency and mud transport ratio, the slag discharge effect is the best when the gas injection rate is 8.4 m^3/h. Taking the optimized model as an example, the slag discharge efficiency is increased by 40.38% and 13.59% respectively compared with the gas injection volume of 6.4 m^3/h and 10.4 m^3/h, and the mud transport ratio is increased by 25.44% and 18.42% respectively.

5.4.3 Air duct sinking ratio

The slag discharge effect when the air duct sinking ratio is 0.70–0.89 m^3/h (Zhang et al.2008; Yin et al.2009) is shown in Fig. 16.

As can be seen from the analysis of Fig. 16a, the displacement of mud and rock slag is positively correlated with the submerged length of the air duct, and the displacement of mud and rock slag in the optimized model is the largest. When the air duct sinking ratio increases from 0.70 to 0.89, the displacement of rock slag and mud in the optimized model increases by 28.35% and 45.02% respectively, and the average displacement of rock slag in the optimized model increases by 20.47% compared with that in the field model. Increasing the submerged length of the air duct can make the two-phase flow of rock slag-slurry be ‘ accelerated by gas injection ‘ in advance, and discharge to the ground at a high flow rate, which effectively reduces the return time of rock slag and slurry in the slag discharge pipe and improves the slag discharge efficiency. Therefore, increasing the buried coefficient of the air duct can effectively improve the discharge capacity of slurry and rock slag.

As can be seen from the analysis of Fig. 16b, slag discharge efficiency and pneumatic conveying ratio are positively correlated with air duct sinking ratio, while mud transport ratio is negatively correlated with it. When the air duct sinking ratio increases from 0.70 to 0.89, the slag discharge efficiency and pneumatic lifting capacity of the field and optimized models increase by 20.56% and 28.37% respectively, while the mud transport ratio decreases by 12.46% and 11.49% respectively. Combined with Fig. 16, considering the discharge capacity and slag discharge index comprehensively, it is considered that the air duct sinking ratio is reasonable when it is 0.84.

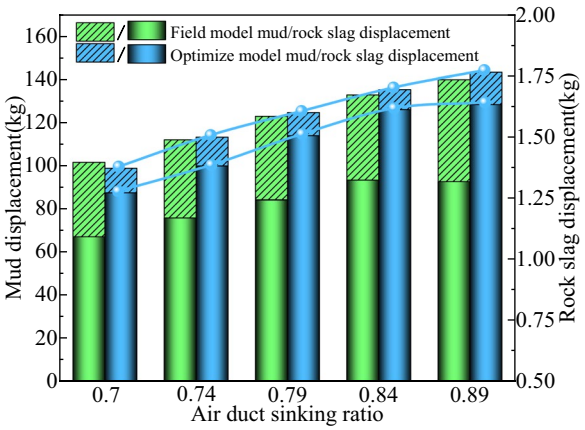

(a) Displacement of rock slag and mud

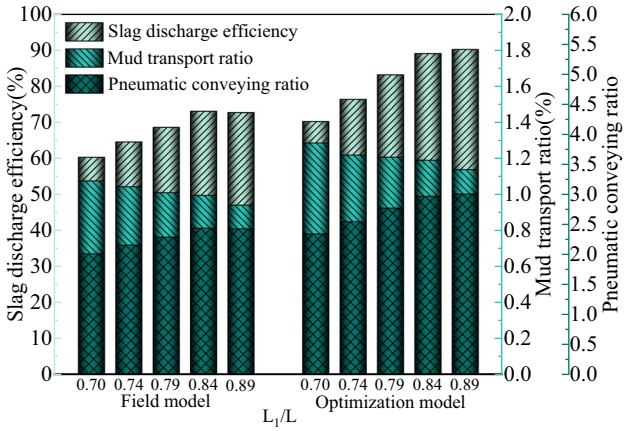

(b) Trend chart of slag discharge index

Fig. 16 Influence of air duct sinking ratio on slag discharge effect of field model and optimization model

5.4.4 Mud viscosity

The slag discharge effect when the mud viscosity is 1–11 mPa·s is shown in Fig. 17.

As can be seen from the analysis of Fig. 17a, increasing the viscosity of mud within a reasonable range can effectively improve the discharge of rock slag, and the viscosity of mud is negatively correlated with the discharge of mud. The mud with low viscosity and low density has poor rock carrying capacity and low discharge of rock slag. When the mud viscosity increases from 1 to 5.5 mPa·s, the rock slag displacement of the optimized model increases by 47.6%. When the mud viscosity continues to increase, the rock slag displacement tends to be stable, while the mud displacement keeps decreasing. Low viscosity mud has little drag and lifting effect on rock slag, and its rock carrying capacity is poor. The wall shear force between high viscosity mud and the inner wall of slag discharge pipe is large, and the friction

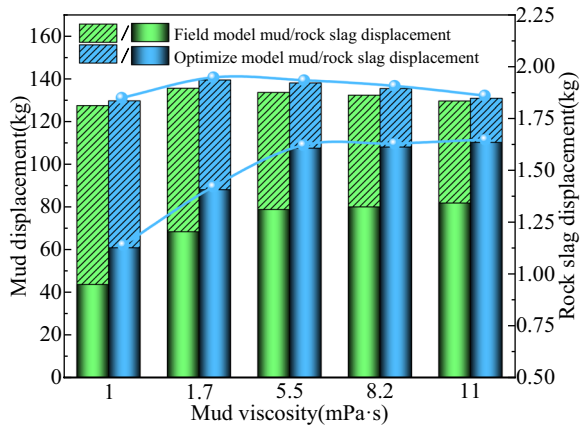

(a) Displacement of rock slag and mud

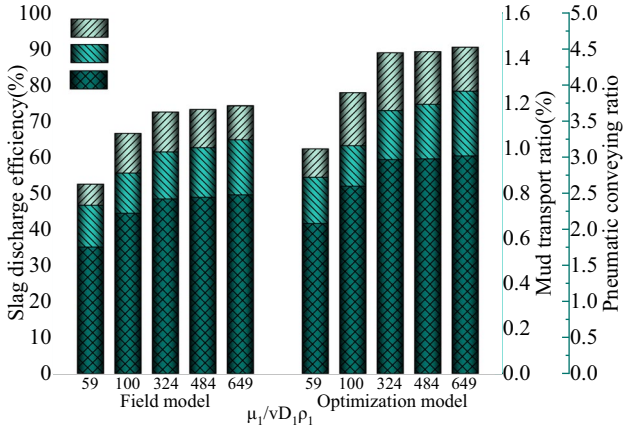

(b) Trend chart of slag discharge index

Fig. 17 Influence of mud viscosity on slag discharge effect of field model and optimized model

loss along the way is serious, so the slag discharge effect cannot be significantly improved, so there is a reasonable threshold for mud viscosity.

As can be seen from the analysis of Fig. 17b, Slag removal efficiency and pneumatic conveying ratio increase greatly at first and then tend to be stable with the increase of mud viscosity. The mud transport ratio is positively correlated with mud viscosity, and the slag removal effect of the optimized model is significantly improved compared with the field model. When the mud viscosity increased from 1 to 11 mPa·s, the slag discharge efficiency of the field and the optimized model increased significantly by 38.09% and 42.67%, respectively, and then nearly stabilized, while the mud transport ratio increased by 38.99% and 43.76%, respectively. Combined with Fig. 17, considering comprehensively the rock carrying capacity and slag discharge effect of mud, it is considered that the mud viscosity is the most reasonable when it is 5.5 mPa·s.

5.4.5 Factor sensitivity analysis

According to the model test results in Sects. 5.4.1 to 5.4.4, the extreme influence of the above factors on the evaluation index of slag discharge effect is obtained, as shown in Table 3:

As can be seen from Table 3, the sensitivity of the four factors to the effect of slag discharge can be attributed to: bit rotation speed w > gas injection volume Q_g > air duct sinking ratio δ > mud viscosity μ_l.

6 Comparison of numerical simulation and experimental results

Based on the visual simulation air-lift reverse circulation slag discharge test device independently developed in Sect. 5.2, the upward velocity of rock slag in the optimized model slag discharge pipe was obtained by PIV monitoring technology (Cheng et al. 2023; Wang et al.2015), and the test results were compared with the numerical simulation results.

As can be seen from the analysis of Fig. 18, The simulation results show that the average upward velocity of rock slag in liquid–solid and liquid–solid–gas sections is 1.76 m/s and 3.42 m/s, 1.79 m/s and 3.47 m/s, 1.77 m/s and 3.34 m/s, 1.82 m/s and 3.52 m/s, respectively, under the influence of four factors: bit rotation speed, gas injection volume, air duct sinking ratio and mud viscosity. The corresponding test results are 1.6 m/s and 3.69 m/s, 1.54 m/s and 3.6 m/s, 1.55 m/s and 3.58 m/s, 1.72 m/s and 3.61 m/s respectively. The relative errors are 10.0% and 7.3%, 16.2% and 3.8%, 14.2% and 6.7%, 5.8% and 2.5% respectively. The simulation

Table 3 Evaluation index range table of slag discharge effect

Influencing factor	Variation range	Extreme range of slag discharge index of field model			Extreme range of slag discharge index of optimized model		
		η	λ	ξ	η	λ	ξ
w	20 ~ 40 r/min	28.16%	0.41%	0.94	37.00%	0.53%	1.24
Q_g	6.4 ~ 10.4 m^3/h	20.87%	0.20%	0.89	25.63%	0.24%	0.93
δ	0.7 ~ 0.88	12.77%	0.13%	0.43	19.94%	0.15%	0.67
μ_l	1.7 ~ 11.0 mPa·s	7.64%	0.15%	0.25	12.57%	0.24%	0.42

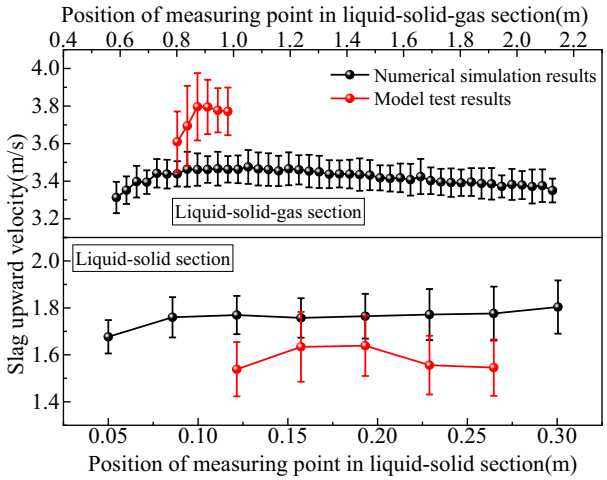

(a) Comparison chart of the influence of bit rotation speed on the upward velocity of rock slag.

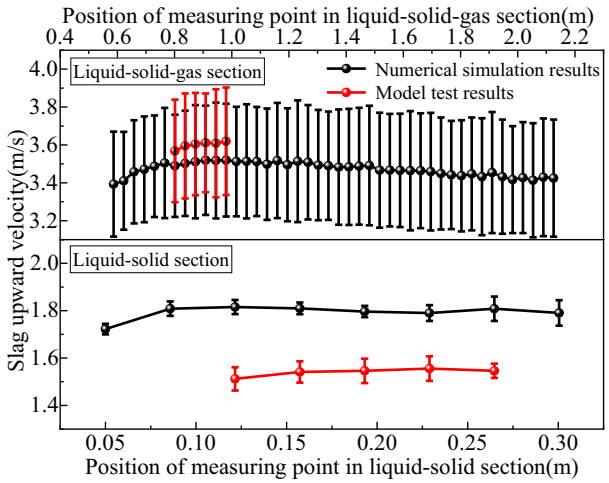

(b) Comparison diagram of the influence of gas injection volume on the upward velocity of rock slag.

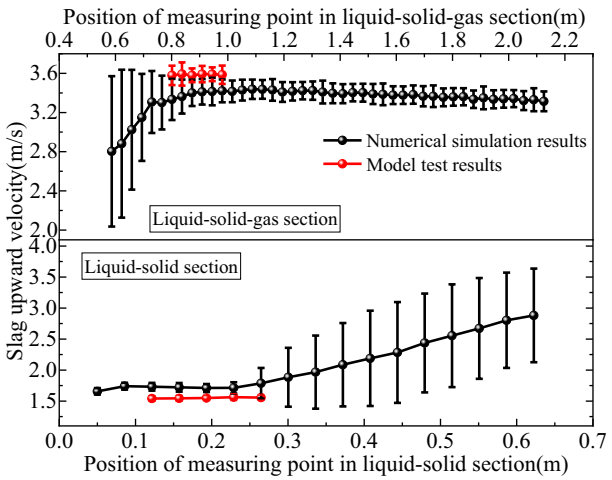

(c) Comparison diagram of the influence of air duct sinking ratio on the upward velocity of rock slag.

Fig. 18 Comparison between numerical simulation and model test results

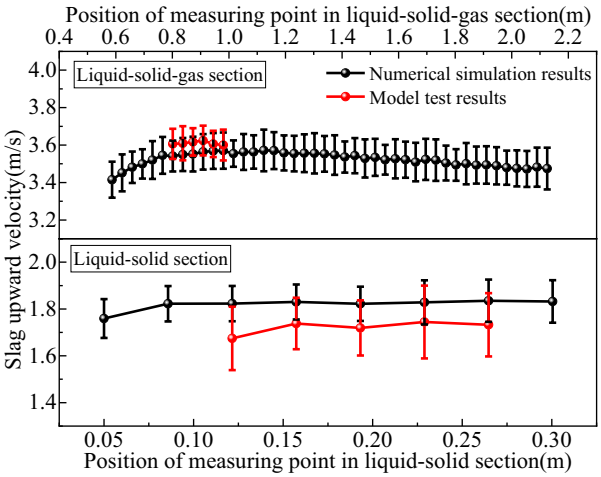

(d) Comparison diagram of the influence of mud viscosity number on the upward velocity of rock slag.

Fig. 18 (continued)

results are in good agreement with the experimental results, which verifies the correctness of the distribution law of gas lift reverse circulation multiphase coupling slag discharge flow field and the reliability of CFD-DEM method, PIV monitoring technology and self-developed slag discharge test device.

7 Discussion

(1) In order to improve the efficiency of slag discharge, we can optimize the drilling construction parameters according to the migration characteristics of rock slag and mud at the bottom of the well and in the slag discharge pipe, improve the ability of gathering and suspending rock slag at the bottom of the well, enhance the adsorption of slag suction port, and strengthen the ability of mud to carry rock and lift it pneumatically, so as to realize the complete clearing of rock slag at the bottom of the well.

(2) Based on the self-developed visual air-lift reverse circulation slag discharge test device, the effects of bit rotation speed, gas injection volume, air duct sinking ratio and mud viscosity on slag discharge effect were analyzed. After similar transformation into actual engineering drilling parameters, the efficient slag discharge process parameters were obtained: bit rotation speed was 8.7 r/min, gas injection volume was 4200 m^3/h, air duct sinking ratio was 0.84 and the mud viscosity was 165 mPa·s.

(3) Under the action of high pressure and grinding, the argillaceous rock layer reacts with the mud, resulting in the change of the properties of rock slag and mud, which is the natural reason for the low drilling efficiency and serious tool wear in the Cretaceous-Jurassic strata in western China. However, the layout of cutter head, slag suction port, bit structure and the selection of drilling construction parameters cannot meet the requirements of efficient drilling, which is the main reason for low drilling efficiency.

8 Conclusions

In order to reveal the distribution law of liquid–solid–gas multiphase coupling slag discharge flow field and the influencing factors of slag discharge effect in gas-lift reverse circulation slag discharge, the numerical model and experimental platform of gas-lift reverse circulation slag discharge were established, the layout of slag suction port of cutter head was optimized, and the distribution law of multiphase coupling slag discharge flow field and the influencing factors of slag discharge effect were analyzed. According to this study, the following conclusions can be drawn:

(1) Based on the numerical model of gas-lift reverse circulation slag discharge, and changing the number, spacing, area ratio and total area of slag suction ports in turn to optimize the layout of slag suction ports, the best layout mode of slag suction ports of drill bit is optimized: the number of slag suction ports is 2, the length-diameter ratio is 0.4, the area ratio is 1, and the total area ratio is 1.94%. This layout mode of slag suction ports improves the shortcomings of insufficient adsorp-

tion force and small adsorption area in the current slag suction port layout center, and the slag removal rate is also higher than that in the field.

(2) The migration of bottom hole fluid is mainly tangential flow, and the axial movement only occurs at the slag suction port, and the radial movement only occurs at both sides of the slag suction port, far away from the slag suction port, so the axial and radial velocity of mud is small, which is easy to cause cuttings accumulation. Rock slag moves in a dynamic cycle of "convergence-suspension-adsorption-lifting" at the bottom of the well. The movement of mud and rock slag in the slag discharge pipe is mainly axial flow, and the velocity increases sharply when passing through the gas injection end.

(3) The rotation speed of the drill bit is negatively correlated with the mud displacement, the gas injection volume and the air duct sinking ratio are positively correlated with the mud displacement. There is an optimal threshold for bit rotation speed and gas injection volume, and each slag discharge index increases first and then decreases with it. Low-density and low-viscosity mud has poor rock carrying capacity and low rock slag discharge.

(4) The combination of construction parameters for high-efficiency slag discharge was proposed: the drill rotation speed is 8.7 r/min, the gas injection volume is 4200 m^3/h, the air duct sinking ratio is 0.84, and the mud viscosity is 165 mPa·s. The sensitivity of the factors affecting the slag discharge effect can be summarized as follows: bit rotation speed w > gas injection volume Q_g > air duct sinking ratio δ > mud viscosity μ_1.

Acknowledgements This research was supported by the National Natural Science Foundation of China (52174104 and 51674006), Key R & D projects in Anhui Province (202004a07020034), and the Graduate Innovation Fund of Anhui University of Science and Technology (2023cx2053and2023cx1006)

Author contribution Longhui Guo: Conceptualization, Data curation, Formal analysis, Writing – original draft. Hua Cheng: Investigation, Supervision, Writing – review & editing. Zhishu Yao: Investigation, Supervision, Writing – review & editing. Chuanxin Rong: Investigation, Supervision, Writing – review & editing. Guang Yang: Data curation. Xiaoyun Wang: Data curation. Yu Fang: Data curation. Bao Xie: Data curation.

Declarations

Competing interests The authors declare that they have no known competing financial interests or personal relationships that could have appeared to influence the work reported in this paper.

References

Adebayo B, Ademola BW (2014) Discontinuities effect on drilling condition and performance of selected rocks in Nigeria. Int J Min Sci Technol 24(5):603–608

Akhshik S, Behzad M, Rajabi M (2016a) CFD-DEM simulation of the hole cleaning process in a deviated well drilling: the effects of particle shape. Particuology 25(2):72–82

Akhshik S, Behzad M, Rajabi M (2016b) Simulation of the interaction between nonspherical particles within the CFD-DEM framework via multisphere approximation and rolling resistance method. Particul Sci Technol 34(4):381–391

Chen H, Tang B, Tang YZ, Yao ZS, Wang CB, Rong CX (2020) Full face tunnel boring machine for deep-buried roadways and its key rapid excavation technologies. J China Coal Soc 45(09):3314–3324

Cheng H, Guo LH, Yao ZS, Wang ZJ, Rong CX (2023) Experimental study on transport law of multiphase slag discharge and optimization of well washing parameters in gas lift reverse circulation of drilling shaft sinking. J China Univ Min Technol 1–14

Cui MY, Liu JY, Li XY, Huang JY (2022) Analysis on mine shaft drilling method applied to mine shaft sinking in Western China area-taking the construction of air inlet shaft in Kekegai coal mine as an example. Min Constr Technol 43(05):67–70

Demirdag S, Sengun N, Ugur I, Efe T, Akbay D, Altindag R (2014) Variation of vertical and horizontal drilling rates depending on some rock properties in the marble quarries. Int J Min Sci Technol 24(2):269–273

Fan Y, Fang Y, Wu PC, Zhong CX, Wang XD, Xia CY (2020) Simulation analysis of cuttings migration in shale gas drilling. Sci Technol Eng 20(28):11532–11538

Fan JD, Feng H, Song CY, Reng HW, Ma Y, Wang QC, Tan J, Liu QH, Li C (2022) Key technology and equipment of intelligent mine construction of whole mine mechanical rock breaking in Kekegai Coal Mine. J China Coal Soc 47(01):499–514

Fan JD, Wei D, Wang QC, Feng H, Liu W, Liu QH, Huang KJ, Yan ZG, Liu JJ, Li C (2023) Theory and practice of intelligent coal mine shaft excavation. J China Coal Soc 48(01):470–483

Fang Y, Yao ZS, Huang XW, Li XW, Diao NH, Hu K, Li H (2022) Permeability evolution characteristics and microanalysis of reactive powder concrete of drilling shaft lining under stress-seepage coupling. Constr Build Mater 331:127336

Hao SQ (2007) Simulation and experimental study on down-the-hole drilling fluid field of the hollow DTH hammer reverse circulation coring and sampling technology. Dissertation, Jilin University.

Huang ZQ, Zhou Y, Shan DW, Yang MJ, Liu SB, Bu Y (2008) Study on influence of layout of DHT bits junk slot on hole-bottom flow field. Equip for Geo Pros 5:296–299

Huang Y (2013) Numerical simulation and experimental study on gas-solid flow field of DTH hammer reverse circulation drilling. Dissertation, Jilin University.

Ji HG, Sun LH, Song CY, Zhang YZ, Wang JH, Meng ZQ (2023) Research progress on stability control of surrounding rock in

weakly cemented strata engineering in western China mining area. Coal Sci Technol 51(01):117–127
Jiao N, Wang YS, Meng CX (2020) Numerical simulation on the flow field and slag carrying efficiency of air flush drilling for vertical shaft boring machine. J China Coal Soc 45(S1):522–531
Kamyab M, Rasouli V (2016) Experimental and numerical simulation of cuttings transportation in coiled tubing drilling. J Nat Gas Sci Eng 29:284–302
Kang HP, Gao FQ, Xu G, Ren HW (2023a) Mechanical behaviors of coal measures and ground control technologies for China's deep coal mines: a review. Int J Rock Mech Min 15(01):37–65
Kang YQ, Yang RS, Yang LY, Li CX, Chen J, Zhu HN, Liu N (2023b) Theoretical and numerical studies of rock breaking mechanism by double disc cutters. Int J Min Sci Technol 33(7):815–828
Liu ZQ, Meng YP (2015) Key technologies of drilling process with raise boring method. Int J Rock Mech Min 7(04):385–394
Liu ZQ, Song CY (2022) The latest development of mechanical rock breaking drilling technology and equipment for large diameter shaft in China. Min Constr Technol 43(01):1–9
Liu SW, Feng YL, Dong SJ (2013) Influence factors analysis and parameters optimization of deslagging in roadway floor anchoring boreholes. J China Univ Mining Technol 42(05):761–765
Liu ZQ, Song CY, Ji HG, Liu SJ, Tan J, Cheng SY, Ning FB (2021) Construction mode and key technology of mining shaft engineering for deep mineral resources. J China Coal Soc 46(03):826–845
Liu JF, He X, Huang HY, Yang JX, Dai JJ, Shi XC, Xue FJ, Timon R (2024) Predicting gas flow rate in fractured shale reservoirs using discrete fracture model and Ga-Bp neural network method. Eng Anal Bound Elem 159:315–330
Meng CX (2019) Study on liquid cleaning system and flow field of vertical shaft boring machin. Dissertation, China University of Mining and Technology.
Oseh JO, Norddin MNAM, Ismail I, Ismail AR, Gbadamosi AO, Agi A (2020) Effect of the surface charge of entrapped polypropylene at nanosilica-composite on cuttings transport capacity of water-based muds. Appl Nanosci 10(01):61–82
Ozbayoglu ME, Miska SZ, Reed (2005) Using foam in horizontal well drilling: a cuttings transport modeling approach. J Petrol Sci Eng 46(4):267–282
Qu JY (2021) Mechanical model of cuttings transport and evaluation of hole cleaning effect in horizontal wells. Dissertation, Northeast Petroleum University.
Shao B, Yan YF, Wang XM, Liao FJ, Yan XZ (2020) Numerical investigation of a double-circulation system for cuttings transport in CBM well drilling using a CFD-DEM coupled model. Eng Appl Comp Fluid 14(1):38–52
Sun LH, Ji HG, Yang BS (2019) Physical and mechanical characteristic of rocks with weakly cemented strata in Western representative mining area. J China Coal Soc 44(03):866–874
Vaziri E, Simjoo M, Chahardowli M (2020) Application of foam as drilling fluid for cuttings transport in horizontal and inclined wells: a numerical study using computational fluid dynamics. J Petrol Sci Eng 194:107325
Wang MS (2007) The parameters optimization of the reverse circulation DTH hammer and studies on its drilling technique. Dissertation, Jilin University.
Wang ZQ, Yang SQ, Peng Z (2011) Knowledge about structure of large diameter ream bit. Min Proce Equip 39(02):40–43
Wang HJ, Liu DA, Gong WL, Li LY (2015) Dynamic analysis of granite rockburst based on the PIV technique. Int J Min Sci Technol 25(2):275–283
Wang Q (2020) Modeling and analysis research of dynamic cuttings transport in extended reach well. Dissertation, Yangtze University.
Xia M, He JJ, Wang ZJ, Song HH (2013) Numerical simulation on flow field of shaft bottom drilled with large-diametered drill bit. Min Proce Equip 41(04):14–19
Xiong L, Zhang XL, Xiong JQ, Yin F (2014) Preliminary analysis on influence factors of air-lift reverse circulation drilling efficiency to large diameter engineering well. Dri Eng 41(05):42–49
Xu D, Liu JF, Liang C, Yang JX, Xu HN, Wang L, Liu J (2024) Effects of cyclic fatigue loads on surface topography evolution and hydro-mechanical properties in natural and artificial fracture. Eng Fall Anal 156:107801
Yan T, Qu JY, Sun XF, Chen Y, Hu QB, Li W, Zhang HX (2020) Numerical investigation on horizontal wellbore hole cleaning with a four-lobed drill pipe using CFD-DEM method. Powder Technol 375(1):249–261
Yao ZH, Wang C, Cheng H, Xue WP, Liang GL (2019) Design optimization and engineering application of high strength shaft lining for rapid construction with drilling shaft sinking method. J China Univ Mining Technol 48(04):742–749
Yao ZS, Fang Y, Qiao SX, Cheng H, Li XW, Wang ZJ, Wang C (2022) Research on backfill technology of drilling shaft sinking method in porous water-bearing rock stratum. Coal Sci Technol 50(10):1–9
Yao ZS, Xu YJ, Cheng H, Fang Y, Wang ZJ, Wang R (2023) Study on the mechanical properties of a new high-strength composite shaft lining for the "one drilling and forming process" by drilling method in western China. J China Coal Soc 1–14
Yin XL, Gao HJ, Yin L (2009) Anti-circulation flushing parameter calculation of the large-diameter shaft drilling. Min Proce Equip 37(21):5–8
Zhang YC, Sun J, Wang AS (2008) Drilling technology. Coal industry press, Beijing
Zhou SH, Li Y, Zhou HW, Kang ZD (2018) Analysis and application of gas lift reverse circulation technology for sediment control of super-long bored pile. Constr Technol 47(24):117–119